Egyptian Journal of Veterinary Sciences

https://ejvs.journals.ekb.eg/

Histopathological and Immunohistochemical Evidence of Curcumin's Defence Against Chlorothalonil Toxicity

Heba M. Elkasaby, Walaa F. Awadin*, Iman Ibrahim and Heba Mahgoub

Department of Pathology, Faculty of Veterinary Medicine, Mansoura University, Mansoura 35516, Egypt

Abstract

CHLOROTHALONIL (Cr), a fungicide widely used worldwide to protect crops from fungal diseases. Curcumin (Cm), a natural antioxidant, was investigated for its protective effects. The experiment involved 120 female Swiss albino mice (weighing 20-25 g), randomly assigned to 12 groups of 10 mice each. Group 1 served as a control. Groups 2 and 3 received Cm at concentrations of 0.5% and 2% in their diet for 12 weeks, respectively. Groups 4, 5, and 6 were administered Cr at doses of 0.1, 10 and 100 mg/kg body weight (B.W.) in their diet for 5 weeks. Groups 7, 8 and 9 were given Cm at 0.5% in their diet for 12 weeks, followed by Cr at 0.1, 10 and 100 mg/kg B.W., respectively, for 5 weeks. Similarly, Groups 10, 11 and 12 received Cm at 2% in their diet for 12 weeks, followed by Cr at 0.1, 10 and 100 mg/kg B.W., respectively, for 5 weeks. At the end of the experiment, all mice were sacrificed, and tissue specimens from the liver, kidneys and spleen were collected, respectively, in their diet for 12 weeks and preserved in 10% neutral buffered formalin for 48 hours for histopathological and immunohistochemical analysis. The results demonstrated that Cm at a 2% concentration provided greater protection than 0.5% in mitigating Cr-induced damage in the examined organs. This protective effect was mediated by increased expression of glutathione peroxidase (GPX) and inhibition of inducible nitric oxide synthase (iNOS), nuclear factor-kappa B (NF-κB) and caspase-3 as observed through immunohistochemistry (IHC).

Key words: Curcumin, Chlorothalonil, IHC.

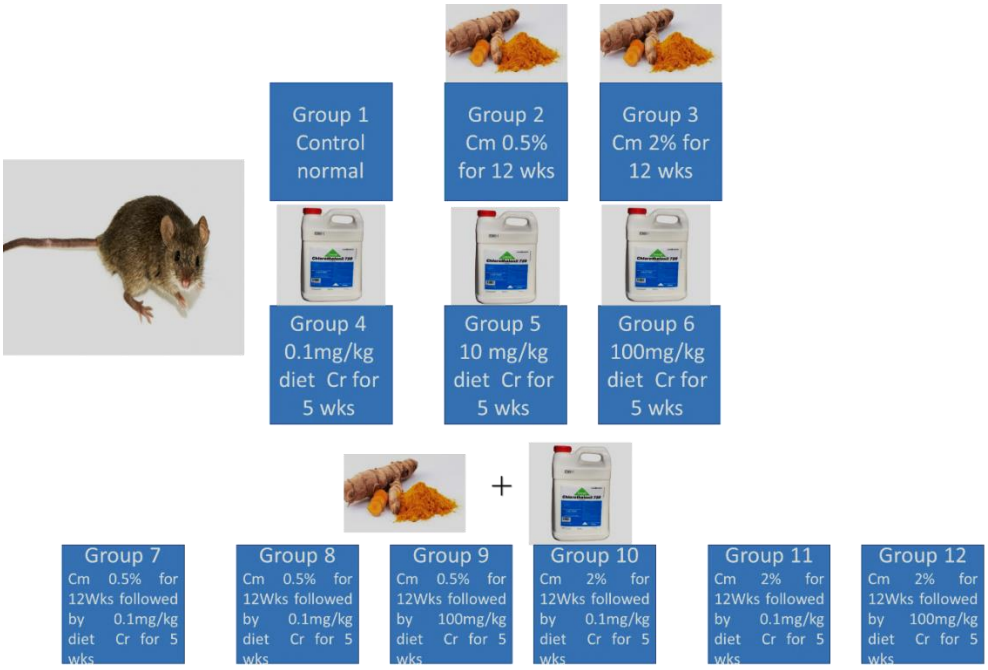

Fig 1. Schematic of experiment design

*Corresponding authors: Walaa F Awadin, E-mail: walaafekriawadin@yahoo.com Tel.: 01024689319
(Received 09 April 2024, accepted 31 May 2025)
DOI: 10.21608/ejvs.2025.373980.2771

Introduction

Chlorothalonil (2,4,5,6-tetrachloro-isophthalonitrile) (Cr) is a non-systemic, broad-spectrum pesticide widely used in agriculture for fungal infection control [1]. It is available in various formulations, including concentrates, powders, and granules [2]. Research indicates that Cr residues in the food chain often exceed maximum permissible levels, posing risks to human health [3]. Cr is known to induce oxidative stress by depleting cellular glutathione (GSH), a crucial molecule in defending against xenobiotics [4]. The depletion of intracellular GSH by Cr results in the dysfunction of GSH-dependent enzymes [5]. Studies have demonstrated that Cr not only inhibits GSH activity [4] but also affects key GSH-related enzymes, such as glutathione peroxidases (GPX), thereby disrupting antioxidant defense systems [6].

Cr adversely impacts organ functions in animals, particularly in the kidneys, triggering cell necrosis and impairing mitochondrial respiration [7]. It inhibits mitochondrial respiratory functions, reduces ATP production, and enhances reactive oxygen species (ROS) generation, ultimately inducing cell necrosis [8]. In contrast, curcumin (Cm), also known as diferuloylmethane, is a natural polyphenol extracted from the rhizome of *Curcuma longa* (turmeric) [9]. As the main active component of turmeric, Cm is recognized for its anti-inflammatory, antioxidant, hepatoprotective, antimicrobial, and tumor-suppressive property [10]. Historically used in many Asian countries as a medicinal herb, feed additive, and coloring agent [11)], Cm has been extensively studied for its pro-apoptotic, chemo preventive, and chemotherapeutic effects.

Glutathione peroxidase (GPX) is a selenium-dependent enzyme that plays a pivotal role in reducing lipid peroxides and hydrogen peroxide, thus mitigating oxidative damage [12]. Nitric oxide (NO), essential for renal functions such as blood flow regulation and glomerular filtration [13], is also a cytotoxic agent involved in inflammatory processes [14]. Nitric oxide synthase (iNOS), an inflammatory mediator, is linked to the pathophysiology of several inflammatory diseases due to excessive NO production [15]. Nuclear factor-kappa B (NF-κB), a key transcription factor, activates inflammatory processes by regulating genes encoding iNOS and proinflammatory cytokines [16,17], including tumor necrosis factor-alpha (TNF-α) [18]. NF-κB activation involves its release from the inhibitory protein IκB through phosphorylation, ubiquitination, and proteasome degradation, ultimately leading to inflammatory cytokine expression [19].

Caspase-3, encoded by the CASP3 gene [20], plays a critical role in apoptosis [21], a process of programmed cell death. It is involved in both the extrinsic (death receptor-mediated) and intrinsic (mitochondria-mediated) apoptotic pathways. Activation of caspase cascades is a key mechanism in initiating apoptosis [22]. This study aims to evaluate the protective effects of Cm on the histopathology of the liver, kidney, and spleen in mice exposed to varying levels of Cr, along with immunohistochemical staining (IHC) to assess GPX, iNOS, NF-κB, and caspase-3 in these organs.

Material and Methods

Experimental animals

Forty female Swiss albino mice (20-25g) were purchased from National research Centre in Dokki, Cairo, Egypt. Animals were kept in special cages at room temperature, under constant conditions of 12-h light/12-h dark cycle with air conditioning and acclimatized for one week before the experiment with free access to mice pellet chow and tap water. Experiment done in Department of Pathology, Faculty of Veterinary Medicine, Mansoura University. Diet was formulated in Department of Animal Nutrition, Faculty of Veterinary Medicine, Mansoura University. Composition of diet (ingredient /kg) for preparation of 30 kg ration as shown in (Table 1) according to [27]**.**

Experiment design

After one week of acclimatization, mice were haphazardly divided into 12 groups of ten mice each as follows:

Group 1: (control group) mice received mice pellet chow and tap water.

Group 2 cm 0.5%: mice received curcumin 0.5% in diet for 12 weeks (purchased from Gerham pharmaceuticals) according to [28]

Group 3 cm 2%: mice received curcumin 2% in diet for 12 weeks (purchased from Gerham pharmaceuticals) according to [28].

Group 4: mice received Cr 0.1mg/kg B.W in diet for 5 weeks. (purchased from Syngenta company)

Group 5: mice received Cr 10 mg/kg B.W in diet for 5 weeks. (purchased from Syngenta company) according to [29].

Group 6: mice received Cr 100 mg/kg B.W in diet for 5 weeks. (purchased from Syngenta company) according to[30].

Group 7: mice received cm 0.5% in diet for 12 weeks followed by Cr 0.1 mg/kg B.W in diet for 5 weeks.

Group 8: mice received cm 0.5% in diet for 12 weeks followed by Cr 10 mg/kg B.W in diet for 5 weeks.

Group 9: mice received cm 0.5% in diet for 12 weeks followed by Cr 100 mg/kg B.W in diet for 5 weeks.

Group 10: mice received cm 2% in diet for 12 weeks followed by Cr 0.1 mg/kg B.W in diet for 5 weeks.

Group 11: mice received cm 2% in diet for 12 weeks followed by Cr 10 mg/kg B.W in diet for 5 weeks.

Group 12: mice received cm 2% in diet for 12 weeks followed by Cr 100 mg/kg B.W in diet for 5 weeks.

Schematic illustration of experiment design was shown in Fig 1.

After end of the experiment, all mice were sacrificed. After gross examination, tissue specimens from liver, kidney and spleen were collected and preserved in 10% neutral buffered formalin for 48 hours for histopathological and immunohistochemical examination.

Histopathological examination

During tissue processing, specimens were trimmed, placed into labeled cassettes, and subjected to dehydration through an ascending series of ethanol concentrations. Clearing was achieved by immersing the specimens in three changes of xylene (1 hour per change), followed by embedding them in paraffin wax. The paraffin blocks were sectioned into four µm-thick slices using a rotary microtome, then deparaffinized in xylene, rehydrated through a descending ethanol series, and stained with hematoxylin and eosin (H&E) following the protocol described in [27]. The stained tissue sections were examined under a light microscope to identify any pathological changes. A semiquantitative scoring system was used to assess degeneration, fibrosis, and inflammation. In the liver, hepatocyte degeneration, fibrosis, and inflammation were scored as follows: 0 (normal), 1 (mild, <25% of affected area), 2 (moderate, 25–50%), and 3 (severe, >50%). Similarly, tubular degeneration, edema, fibrosis, and inflammation in the kidneys, as well as depletion, fibrosis, and hemorrhage in the spleen, were scored using the same scale. A total histopathological score was calculated for each organ [28].

Immunohistochemistry (IHC)

In this study, the expression of GPX, iNOS, NF-κB, and caspase-3 was assessed following the protocols provided by the manufacturers. A total of 144 paraffin-embedded slides were prepared from liver, kidney, and spleen tissues. Tissue sections were immersed in xylene for 20 minutes, followed by an alcohol gradient (50–100%) for rehydration, and then incubated in a 3% hydrogen peroxide (H_2O_2) solution for 10 minutes. After washing in phosphate-buffered saline (PBS), the sections were heated for 4–5 minutes in citrate buffer (pH 6) using an 800-watt microwave, then incubated with a blocking substance for 20 minutes to prevent nonspecific background staining, followed by another PBS rinse.

Subsequently, the tissue sections were incubated overnight in a humidity chamber with specific antibodies, including anti-glutathione peroxidase 4 Rabbit pAb (GB114327, Servicebio, 1:500 dilution), iNOS Rabbit pAb (A0312, 1:500 dilution), NF-κB p65/RelA Rabbit pAb (A2547, Abclonal, 1:200 dilution), and anti-active Caspase-3 Rabbit polyclonal antibody (bs-2072R, Servicebio, 1:1000 dilution). The slides were rinsed in PBS and treated with 4–5 drops of secondary antibody for 10 minutes at room temperature, followed by further rinsing in PBS. Next, the sections were incubated with streptavidin-peroxidase solution for 10 minutes and rinsed in PBS again. For visualization, a chromogen solution of 3–3′-diaminobenzidine tetrahydrochloride (DAB) was applied for 15 minutes. Finally, the sections were counterstained with Mayer's hematoxylin, dehydrated using an alcohol series, and mounted with di-n-butyl-phthalate-polystyrene-xylene (DPX). The staining intensity was graded on a scale of 0 (no signal), 1 (weak), 2 (moderate), and 3 (strong).

Statistical analysis

The revealed data of lesional scores and IHC staining intensity scores were tested for the statistical significance using the software GraphPad prism (www.graphpad.com). Using Kruskal-Wallis and Mann-Whitney U tests; n = 4. Different letters

indicate statistically significant when p-value was <0.05.

Results

Microscopic examination of HE stained liver sections from different treatment groups (Fig.2 A-N) showing normal histological appearance of hepatic parenchyma in Group 1 (A), Group 2 (B) and Group 3 (C). Liver of Group 4 (D) showing diffuse hepatic vacuolation with focal inflammatory foci. The inflammatory foci consisted of aggregations of mild numbers of lymphocytes and plasma cells. Liver of Group 5 (E&F) showing increased lesions consisted of vacuolation of hepatocytes, portal fibrosis admixed with leukocytic cells infiltrates and portal edema, focal necroinflammatory foci. Liver of Group 6 (G&H) showing more severe lesions consisted of multifocal coalescing leukocytic cells aggregation (abundant neutrophils, few lymphocytes and macrophages) replacing necrotic hepatocytes, expansion of portal area with fibrosis, edema, lymphocytes, plasma cells and macrophages infiltration, the adjacent hepatocytes showing mild to moderate intracellular fat vacuoles. Liver of Group 7 (I) showing few intracytoplasmic microvesicular vacuoles, few focal or scattered inflammatory cells consisting of mild numbers of neutrophils, lymphocytes and plasma cells. Liver of Group 8 (J) showing moderate hepatocellular swelling with focal mild perivascular inflammatory foci. Liver of Group 9 (K) showing moderate hepatocellular swelling with few focal to multifocal inflammatory cells consisting of lower numbers of neutrophils, lymphocytes and macrophages. Liver of Group 10 (L) showing few focal inflammatory aggregates. Liver of Group 11 (M) showing multifocal inflammatory foci composed of few macrophages, lymphocytes and rare neutrophils, mildly congested central vein. Liver of Group 12 (N) shows moderate hepatocellular swelling with mildly congested central vein.

Microscopic examination of HE stained kidney sections from different treatment groups (Fig.3 A-O) showing normal histological appearance of glomerulus and renal tubules in (A) Group 1. (B) Group 2 and C) Group 3. Kidney of Group 4 (D) showing mild congestion in intertubular blood vessels, mild tubular necrosis characterized by eosinophilia and pyknotic nuclei. Kidney of Group 5(F&G) showing increased lesions consisted of congestion with mild hemorrhage, interstitial edema, severe tubular dilation, vacuolation degeneration in tubular epithelium and mild tubular necrosis besides inflammatory cells infiltration in interstitial tissue. An early sign of tubular regeneration characterized by overcrowded nuclei was also seen. Kidney of Group 6 (H) showing severe dense interstitial fibrosis admixed with extensive cellular infiltrates besides congestion. Kidney of Group 7(I&J) showing mild tubular dilation, mild congestion, mild tubular necrosis. Kidney of Group 8 (K) showing mild tubular dilation and necrosis. Kidney of Group 9 (D) showing mild tubular dilation, congestion and few inflammatory cells infiltration in interstitial tissue. Kidney of Group 10 (M) showing very mild congestion and very mild tubular vacuolar degeneration. Kidney of Group 11 (N) showing very mild congestion with sign of tubular regeneration characterized by overcrowded nuclei. Kidney of Group 12 (O) showing moderate tubular dilation with sign of tubular regeneration characterized by overcrowded nuclei.

Microscopic examination of HE stained spleen sections from different treatment groups showing normal splenic parenchyma with large well defined lymphoid follicles, normal red pulp containing few megakaryocytes in Group 1 (A), Group 2(B) and Group 3 (C). Spleen of Group 4 (D&E) showing focal area of hemorrhage, decrease in size and number of periarteriolar lymphatic sheaths and lymphoid follicles, fibrous connective tissue proliferation and edema in red pulp. Spleen of Group 5 (F) showing severe lymphoid depletions with lymphocytolysis and necrosis of megakaryocytes. Spleen of Group 6 (G & H) showing loss of lymphoid follicle arrangement with marked degeneration and clumping of lymphocytes and megakaryocytes leaving clear spaced and admixed with abundant scattered RBCs. Spleen of Group 7(I & J) showing slightly enlarged lymphoid follicles with increase the numbers of megakaryoblasts, scattered RBCs with mild fibrosis in red pulp. Spleen of Group 8 (K) showing presence of moderate numbers of megakaryoblasts. Spleen of Group 9 (L) showing restored size of lymphoid follicles with moderate numbers of megakaryocytes. Spleens of Group 10 (M), Group 11 and (N) Group 12 (O) showing well-organized restored size of lymphoid follicles with presence of many megakaryocytes in red pulp.

Collectively, hepatic, renal and splenic lesions increased with increasing dose of Cr exposure in all groups, however, these lesions were less severe in the protected groups with 2% Cm than in unprotected group and the protected groups with 0.5% Cm.

Statistical analysis of histopathological lesional scores (Fig.5) in liver (A) kidney (B) and spleen (C) were lower in protected groups with 2% cm than in unprotected group and protected groups with 0.5% cm.

IHC expression of GPX, INOs, NF-κB and caspase-3 in liver

GPx expression and localization in immunostained liver sections of different treatment groups demonstrated in (Fig. 6 A1-L1). A1) Livers of Group 1, B1) Group 2 and C1) Group 3 showing negative reaction. D1) Livers of Group 4, E1) Group 5and F) Group 6 showing decreased immunopositive sinusoidal reaction with increased Cr dose. G1) Livers of Group 7 H1) Group 8 and I1) Group 9 showing decreased immunopositive sinusoidal reaction with increased Cr dose. J1) Livers of Group 10, K1) Group 11 and L1) Group 12 showing decreased immunopositive sinusoidal reaction with increased Cr dose but appear higher than observed in unprotected group and protected groups with cm0.5%.

iNos expression and localization in immunostained liver sections of different treatment groups demonstrated in (Fig. 6 A2-L2). A2) Livers of Group 1, B2) Group 2 and C2) Group 3 showing negative reaction. D2) Livers of Group 4, E2) Group 5 and F2) Group 6 showing increasing immunopositive reaction in hepatocytes with increased Cr dose. G2) Livers of Group 7, H2) Group 8 and I2) Group 9 showing increasing immunopositive reaction in hepatocytes. J2) Livers of Group 10, K2) Group 11 and L2) Group 12 showing increased immunopositive reaction in hepatocytes with increased Cr dose but appears lower than in unprotected group and protected groups with cm0.5%.

NF-κB expression and localization in immunostained liver sections of different treatment groups demonstrated in (Fig. 7 A1-L1). A1) Livers of Group 1, B1) Group 2 and C1) Group 3 showing few positively stained sinusoidal nuclei. D1) Livers of Group 4, E1) Group 5 and F1) Group 6 showing increasing immunopositive stained sinusoidal nuclei with increased Cr dose. G1) Livers of Group 7, H) Group 8 and I1) Group 9 showing increasing immunopositive stained sinusoidal nuclei with increased Cr dose. J1) Livers of Group 10, K1) Group 11 and L1) Group 12 showing increased positively stained sinusoidal nuclei with increased Cr dose however still lower than observed in unprotected group and protected groups with cm0.5%.

Caspase-3 expression and localization in immunostained liver sections of different treatment groups demonstrated in (Fig. 7 A2-L2). A2) Livers of Group 1, B2) Group 2 and C2) Group 3 showing negative reaction. D2) Livers of Group 4, E2) Group 5 and F2) Group 6 showing increasing immunopositive reaction in hepatocytes with increased Cr dose. G2) Livers of Group 7 H2) Group 8 and I2) Group 9 showing increasing immunopositive reaction in hepatocytes. J2) Livers of Group 10, K2) Group 11 and L2) Group 12 showing lower immunopositive reaction in hepatocytes than in unprotected group and protected groups with cm0.5%.

IHC expression of GPX, INOs, NF-κB and caspase-3 in kidneys

GPx expression and localization in immunostained kidney sections of different treatment groups demonstrated in (Fig. 8A1-L1). Kidneys of A1) Group 1, B1) Group 2 and C1) Group 3 showing strong immunopositive interstitial reaction. D1) Kidneys of Group 4, E1) Group 5 and F1) Group 6 showing decreasing immunopositive interstitial reaction with increased Cr dose. G1) Kidneys of Group 7 H1) Group 8 and I1) Group 9 showing decreasing immunopositive interstitial reaction with increased Cr dose. J1) Kidneys of Group 10, K1) Group 11 and L1) Group 12 showing decreased immunopositive interstitial reaction but still higher than observed in unprotected group and protected groups with cm 0.5%.

iNos expression and localization in immunostained kidney sections of different treatment groups demonstrated in (Fig. 8 A2-L2). A2) Kidneys of Group 1, B2) Group 2 and C2) Group 3 showing very mild immunopositive tubular reaction. D2) Kidneys of Group 4, E2) Group 5 and F) Group 6 showing increasing immunopositive tubular reaction with increased Cr dose. G2) Kidneys of Group 7 H2) Group 8 and I2) Group 9 showing increasing immunopositive tubular reaction with increased Cr dose. J2) Kidneys of Group 10, K2) Group 11 and L2) Group 12 showing increased immunopositive tubular reaction with increased Cr dose but still lower than observed in unprotected group and protected groups with cm0.5%.

NF-κB expression and localization in immunostained kidney sections of different treatment

groups demonstrated in (Fig. 9 A1-L1). A1) Kidneys of Group 1, B1) Group 2 and C1) Group 3 showing mild immunopositive nuclear reaction in tubules. D1) Kidneys of Group 4, E1) Group 5 and F1) Group 6 showing increasing immunopositive nuclear reaction in tubules with increased Cr dose. G1) Kidneys of Group 7 H1) Group 8 and I1) Group 9 showing increasing immunopositive nuclear reaction in tubules with increased Cr dose. J1) Kidneys of Group 10, K1) Group 11 and L1) Group 12 showing increasing nuclear reaction in tubules with increased Cr dose however appear less than the reaction observed in unprotected group and protected groups with cm0.5%.

Caspase-3 expression and localization in immunostained kidney sections of different treatment groups demonstrated in (Fig. 9A2-L2). A2) Kidneys of Group 1, B2) Group 2 and C2) Group 3 showing negative reaction. D2) Kidneys of Group 4, E2) Group 5 and F2) Group 6 showing increasing immunopositive tubular reaction with increased Cr dose. G2) Kidneys of Group 7 H2) Group 8 and I2) Group 9 showing increasing immunopositive tubular reaction. J2) Kidneys of Group 10, K2) Group 11 and L2) Group 12 showed lower immunopositive tubular reaction than in unprotected group and protected groups with cm0.5%.

IHC expression of GPX, INOs, NF-κB and caspase-3 in spleen

GPx expression and localization in immunostained spleen sections of different treatment groups demonstrated in (Fig. 10 A1-L1). Spleen of A1) Group 1, B1) Group 2 and C1) Group 3 showing strong immunopositive reaction in lymphocytes. D1) Spleen of Group 4, E1) Group 5 and F1) Group 6 showing decreasing immunopositive reaction in lymphocytes with increased Cr dose. G1) Spleen of Group 7 H1) Group 8 and I1) Group 9 showing decreasing immunopositive reaction in lymphocytes with increased Cr dose. J1) Kidneys of Group 10, K1) Group 11 and L1) Group 12 showing decreased immunopositive reaction in lymphocytes but still higher than observed in in unprotected group and protected groups with cm0.5%.

iNos expression and localization in immunostained spleen sections of different treatment groups demonstrated in (Fig. 10 A2-L2). A2) Spleen of Group 1, B2) Group 2 and C2) Group 3 showing mild immunopositive reaction in lymphocytes. D2) Spleen of Group 4, E2) Group 5 and F) Group 6 showing increasing immunopositive reaction in lymphocytes with increased Cr dose. G2) Spleen of Group 7 H2) Group 8 and I2) Group 9 showing increasing immunopositive reaction in lymphocytes with increased Cr dose. J2) Spleen of Group 10, K2) Group 11 and L2) Group 12 showing increased immunopositive reaction in lymphocytes with increased Cr dose but still lower than observed in in unprotected group and protected groups with cm0.5%.

NF-κB expression and localization in immunostained spleen sections of different treatment groups demonstrated in (Fig. 11 A1-L1). A1) Spleen of Group 1, B1) Group 2 and C1) Group 3 showing negative reaction. D1) Spleen of Group 4, E1) Group 5 and F1) Group 6 showing increasing immunopositive reaction in lymphocytes with increased Cr dose. G1) Spleen of Group 7 H) Group 8 and I1) Group 9 showing increasing immunopositive reaction in lymphocytes with increased Cr dose. J1) Spleen of Group 10, K1) Group 11 and L1) Group 12 showing increased immunopositive reaction in lymphocytes with increased Cr dose but still lower than observed in in unprotected group and protected groups with cm0.5%.

Caspase-3 expression and localization in immunostained spleen sections of different treatment groups demonstrated in (Fig. 11A2-L2). A2) Spleen of Group 1, B2) Group 2 and C2) Group 3 showing negative reaction. D2) Spleen of Group 4, E2) Group 5 and F2) Group 6 showing increasing immunopositive reaction in lymphocytes with increased Cr dose. G2) Spleen of Group 7 H2) Group 8 and I2) Group 9 showing increasing immunopositive reaction in lymphocytes. J2) Spleen of Group 10, K2) Group 11 and L2) Group 12 showing increased immunopositive reaction in lymphocytes with increased Cr dose but still lower than observed in unprotected group and protected groups with cm0.5%.

Semi-quantitative scoring of GPX, i-Nos, NF-κB and caspase-3 in liver, kidney and spleen (Fig. 12A-D) were expressed as Mean±SEM. Statistical analysis of immunostaining scores were lower in protected groups with 2% cm than in unprotected group and protected groups with 0.5% cm.

Discussion

The high demand for food production has been led to increased use of pesticide [29]. While pesticides play an important role in the effort to

overcome plant losses caused by different types of pests to increase food production, at the same time, they can cause several environmental hazards due to their toxicities and accumulation in the environment [30]. Pesticide residues were detected in human and animal food have an adverse effect on general health [31]. Cr is a non-systemic fungicide ,widely applied in agriculture for crop protection due to its biocidal effect and incorporated in many useful aspects [32]. Cr is ranked as a grade III or moderately toxic chemical [33].The spleen is the site of direct and indirect toxicity, a target for some carcinogens, and also a site for metastatic neoplasia[34]. Therefore, we examined the effect of exposure of female mice to different levels of Cr in liver, kidney and spleen and the protective effect of Cm. Necroinflammatory lesions were observed in liver and kidney that increased in severity by increasing levels of Cr exposure. Very similar findings were reported by[35]**.** Cm 2% for 12 weeks was able to maintain liver and kidney tissue structures to some extent in female Swiss albino mice exposed to Cr. These finding were consistent with those noticed by [36] when male Wistar rat fed Cm orally (80 mgkg-1 b.w.). Also, [37] proved the hepato and nephroprotective effect of Cm in female albino rats orally administrated 80 mg/kg b.w. Cm daily for 30 days. The spleen contains hematopoietic and lymphoid elements, is a primary site of extramedullary hematopoiesis, and removes degenerate and aged red blood cells as well as particulate materials and circulate bacteria from the blood supply. Lesions of this important component of the immune system may center on the red pulp, the white pulp or involve both compartments [34]. Our findings in spleen of unprotected Cr groups showed decrease in size and number of periarteriolar lymphatic sheaths and lymphoid follicles, fibrous connective tissue proliferation and edema in red pulp. In addition, lymphoid depletions with lymphocytolysis and necrosis of megakaryocytes were recorded. Toxic compounds induced lymphocyte toxicity and necrosis of the white pulp as mentioned by[34].

Megakaryocytes indicated extramedullary hematopoiesis that present in spleen of normal rodents, especially in mice, more commonly in young compared to aged rodents and, more common in females compared to males[34]. Spleen of Cm protected groups showed restored size of lymphoid follicles and increased numbers of megakaryoblasts.

Generally, pesticides known to induce regeneration of ROS which cause damage vital molecules as lipids, proteins and nucleic acids in living tissue [38]. Several studies documented Cr ability to induce oxidative stress, increase ROS and interruption of anti-oxidant enzymes activity [39]. Our IHC results proved that Cr decreased activity of GPx in all examined organs and thus increased rate of oxidative damage. These results were in line with those proven by [40]in which treatment of CIK cells with Cr 5 µg/L for 48 h resulted in decrease activity of GPx and stimulation of oxidative stress. In our study, Cm increased the immunostaining of GPX which proves its anti-oxidant effect. These results were in line with those documented by [41] in which male rats received Cm orally for 5 weeks 15mg/kg body weight and results were restoration of GSH levels after aflatoxin B1-intoxicated rats and increase activities of GPX. Cm acts as a powerful scavenger of free radicals as ROS and reactive nitrogen species [42]. ROS is considered the major cause of cell damage during chronic diseases such as diabetes mellitus, cancer, cardiovascular disorders and others [43]**.** Cr induced inflammation in liver and kidney through increasing immunostaining of iNos and NF-κB in three examined organs in a dose dependent manner. Previous studies have been shown that chemical pesticides play a vital role in induction of inflammatory response as a part of its mechanism of action [44]. Inflammation and oxidative stress are closely linked to each other's in which the oxidative stress can be caused by the reactive species released by inflammatory cells at the site of inflammation [45]. One of the most important transcription factors is NF-κB which act as potent regulator of inflammatory process [46]. Cm acts as a potent blocker of NF-κB activation [47]. Our IHC findings reported lower immunostaining of iNOS and NF-κB in three examined organs in protected group Cm2% than in Cm0.5%.

Oral administration of Cm as a protective tool before Cr administration has led to decreasing damaging effect of Cr through inhibition of iNOS production to some extent and thus protection of organ from its cytotoxic effect. These findings agreed with those concluded by [48] who proven that Cm treatment (200 mg/kg body weight) decreased iNOS expression in a time dependent manner (7,15,30 days) after intoxication of Male albino Wistar rats with gentamicin for six consecutive days. Cm also has the ability to interfere with NO production and iNOS expression through direct inhibition of NF-κB activation [49].

In addition, our results showed increasing

expression of caspase-3 in liver, kidney and spleen by increasing levels of Cr exposure indicating activation of apoptosis process as mentioned by. Exposure of *Ctenopharyngodon idellus* (grass carp) and kidney cell line to Cr (98%) then analysis by AO-EB staining and flow cytometry induced caspase-3 expression [50]. The protective and anti-apoptotic effect of Cm on APAP induced hepatic toxicity was confirmed by [51] when male BALB/c mice (6-8 wks. of age) intraperitoneally injected with Cm (10 or 20 mg/kg) 2 hours before injection of APAP. Pretreatment with Cm resulted in stimulation of Bcl-2 expression (anti-apoptotic protein) and inhibition of expression of Bax (pro-apoptotic protein) in liver [51]. Depending on these results, we can demonstrate that CUR decreases caspase-3 expression as a result of inhibition of apoptotic pathway at all as caspase-3 is critical activator of apoptotic pathway.

Conclusion

The severity of histopathological lesions in the liver, kidneys, and spleen was found to increase with higher levels of Cr exposure, while these lesions were notably reduced in the group protected with 2% Cm (Cm2%) compared to the unprotected group and the group receiving 0.5% Cm (Cm0.5%). Immunohistochemical (IHC) analysis revealed mild immunostaining for GPX but marked immunostaining for iNOS, NF-κB, and caspase-3 across the examined organs in the unprotected group. In contrast, the group protected with Cm2% exhibited stronger GPX immunostaining alongside reduced immunostaining for iNOS, NF-κB, and caspase-3, indicating the enhanced protective effect of Cm 2% over Cm 0.5% in mitigating Cr-induced damage.

The Acknowledgment

We appreciate all those who contributed to supporting this research.

Conflicts of interest

The authors declare no conflict of interest.

Funding statement

Self-funding.

Ethics approval

This research was approved by the Ethical Committee, Faculty of Veterinary Medicine, Mansoura University, Egypt under code number (M/113).

TABLE 1. Ingredients of animal ration

Ingredients %	%
Yellow corn 8.5%	71.5
Soyabean meal 44%	18
Sunflower oil	4
Corn gluten	1
Minerals and Vitamins	0.25
Di Calcium phosphate	2.5
Limestone	1.2
NaCl salt	0.5
Methionine	0.5
Lysine	0.5

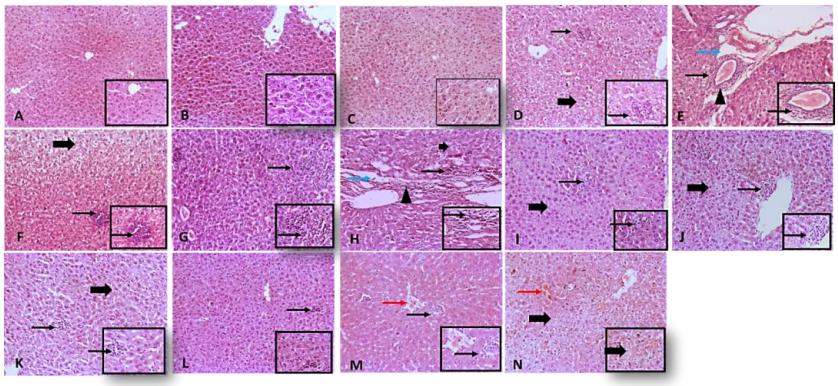

Fig 2. Representative photomicrograph of HE stained liver sections from different treatment groups. A) Livers of Group 1, B) Group 2 and C) Group 3 showing normal histological appearance of hepatic parenchyma. D) Liver of Group 4 showing diffuse vacuolation of hepatocytes with focal inflammatory foci (thick arrow), insert, the inflammatory foci consisted of aggregations of mild numbers of lymphocytes and plasma cells (thin black arrow). E) Liver of Group 5 showing hepatic vacuolation (thick arrow) with portal fibrosis (arrowhead) admixed with leukocytic cells infiltrates (thin black arrow) and portal edema (thin blue arrow), insert, aggregations of lymphocytes, plasma cells and macrophages. F) Liver of Group 5 showing moderate to severe hepatocellular swelling (thick arrow) with focal necroinflammatory foci (thin black arrow), inset, aggregation of lymphoplasmacytic cells and neutrophils focally replacing and surrounding necrotic hepatocytes. G) Liver of Group 6 showing scattered leukocytic cells aggregates (thin black arrow) consisted of abundant neutrophils, few lymphocytes and macrophages replacing necrotic hepatocytes, inset, the leukocytic cells aggregates. H) Liver of Group 7 showing moderate expansion of portal area with fibrosis (arrowhead), edema (thin blue arrow) lymphocytes, plasma cells and macrophages infiltration, the adjacent hepatocytes showing mild to moderate intracellular fat vacuoles. I) Liver of Group 7 showing few intracytoplasmic microvesicular vacuoles (thick arrow) with few focal or scattered inflammatory cells consisted of mild numbers of neutrophils, lymphocytes and plasma cells (thin black arrow), inset. J) Liver of Group 8 showing moderate hepatocellular swelling with focal mild perivascular inflammatory foci. K) Liver of Group 9 showing moderate hepatocellular swelling (thick arrow) with few focal to multifocal inflammatory cells (thin black arrow) consisted of low numbers of neutrophils, lymphocytes and macrophages. L) Liver of Group10 showing few focal inflammatory aggregates (thin black arrow). M) Liver of Group 11 showing multifocal inflammatory foci (thin black arrow) composed of few macrophages, lymphocytes and rare neutrophils, mildly congested central vein (red arrow). N) Liver of Group 12 showing moderate hepatocellular swelling (thick arrow) with mildly congested central vein (red arrow). Low magnification= 100x, high magnification=400x.

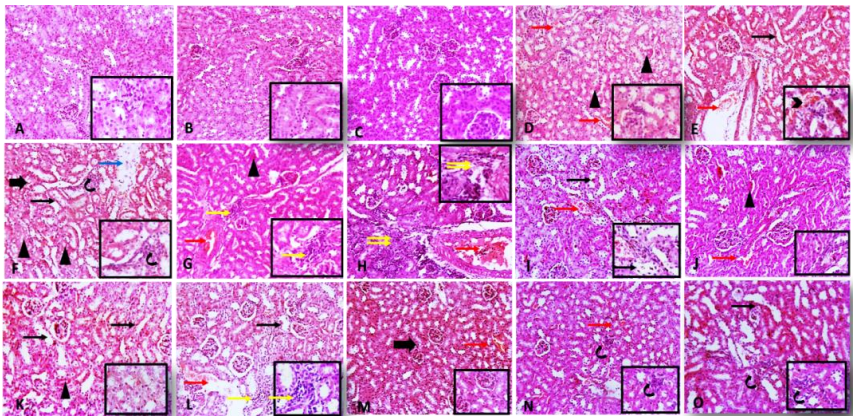

Fig 3. Representative photomicrograph of HE stained kidney sections from different treatment groups. Kidney of A) Group 1, B) Group 2 and C) Group 3 showing normal histological appearance of glomerulus and renal tubules. D) Kidney of Group 4 showing mild congestion (red arrow) in intertubular blood vessels, mild tubular necrosis (closed arrowheads) characterized by eosinophilia and pyknotic nuclei E) and F) Kidney of Group 5 showing congestion (red arrow) and mild hemorrhage (open arrowhead), interstitial edema (blue arrow), severe tubular dilation (thin black arrow), vacuolation degeneration in tubular epithelium (thick arrow) and necrosis in tubular epithelium (closed arrowheads). An early sign of tubular regeneration characterized by overcrowded nuclei (curved arrow) is seen. G) Kidney of Group 5 showing congestion (red arrow), inflammatory cells infiltration in interstitial tissue (yellow arrow) with mild tubular necrosis (closed arrowheads). H) Kidney of Group 6 showing severe dense interstitial fibrosis admixed with extensive cellular infiltrates (double yellow arrow) besides congestion (red arrow). I) and J) Kidney of Group 7 showing mild tubular dilation (thin black arrow), mild congestion (red arrow), mild tubular necrosis (closed arrowheads). K) Kidney of Group 8 showing mild tubular dilation (thin black arrow) and necrosis (closed arrowhead). L) Kidney of Group 9 showing mild tubular dilation (thin black arrow), congestion (red arrow) and few inflammatory cells infiltration in interstitial tissue (yellow arrow). M) Kidney of Group 10 showing very mild congestion (red arrow) and very mild tubular vacuolar degeneration (thick arrow). N) Kidney of Group 11 showing very mild congestion (red arrow) with sign of tubular regeneration characterized by overcrowded nuclei (curved arrow). O) Kidney of Group 12 showing moderate tubular dilation (thin black arrow) with sign of tubular regeneration characterized by overcrowded nuclei (curved arrow). Low magnification= 100x, high magnification=400x.

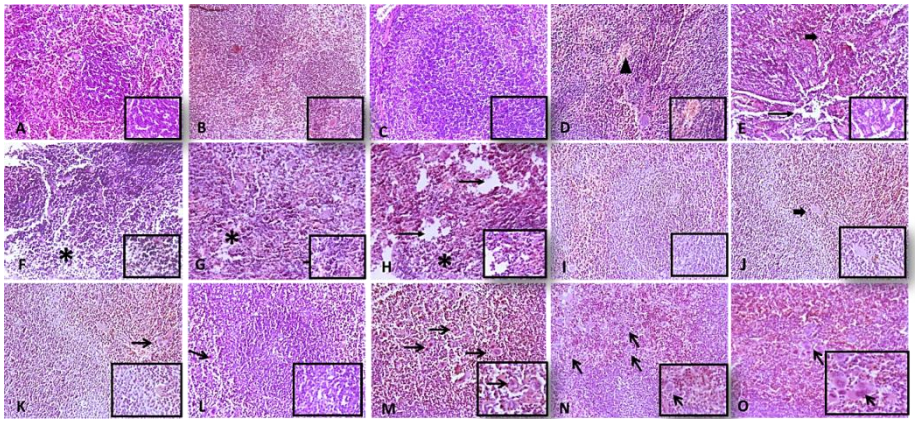

Fig 4. Representative photomicrograph of HE stained spleen from different treatment groups. Spleen of A) Group 1, B) Group 2 and C) Group 3 showing normal well defined lymphoid follicles and red pulp. D) Spleen of Group 4 showing focal area of hemorrhage (arrowhead), decrease in size and number of periarteriolar lymphatic sheaths and lymphoid follicles. E) Spleen of Group 4showing fibrous connective tissue proliferation (thick arrow) and edema (thin black arrow). F) Spleen of Group 5 showing severe lymphoid depletions with lymphocytolysis (*) and necrosis of megakaryocytes. G) and H) Spleen of Group 6 showing loss of lymphoid follicle arrangement with marked degeneration (*) and clumping of lymphocytes and megakaryocytes leaving clear spaced (thin black arrow) and admixed with abundant scattered RBCs. I) and J) Spleen of Group 7 showing slightly enlarged lymphoid follicles with increase the numbers of megakaryoblast and presence of scattered RBCs with mild fibrosis (thick arrow) in red pulp. K) Spleen of Group 8 showing presence of moderate numbers of megakaryoblasts. L) Spleen of Group 9 showing restored size of lymphoid follicles with moderate numbers of megakaryocytes. M) Spleen of Group10, N) Group 11 and O) Group 12 showing well-organized restored size of lymphoid follicles with many megakaryocytes. Low magnification= 100x, high magnification=400x.

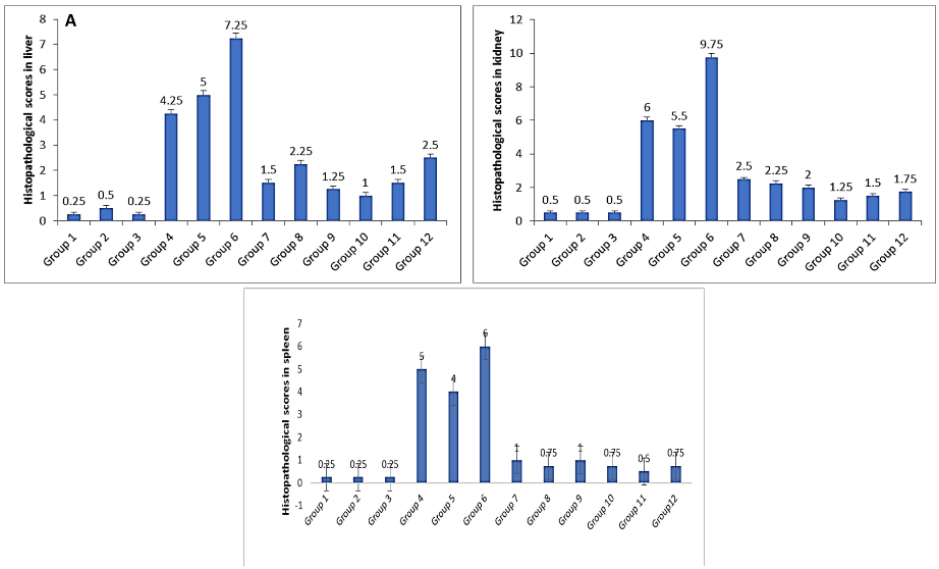

Fig 5. Statistical analysis of histopathological lesional scores in liver (A) kidney (B) and spleen (C) showing lower histopathological scores showing increasing histopathological scores with increasing Cr exposure level. Lower histopathological scores achieved in groups protected with 2% cm than observed in unprotected groups protected groups with 0.5% cm. in three examined organs in groups protected with 2% cm than observed in protected groups with 0.5% cm.

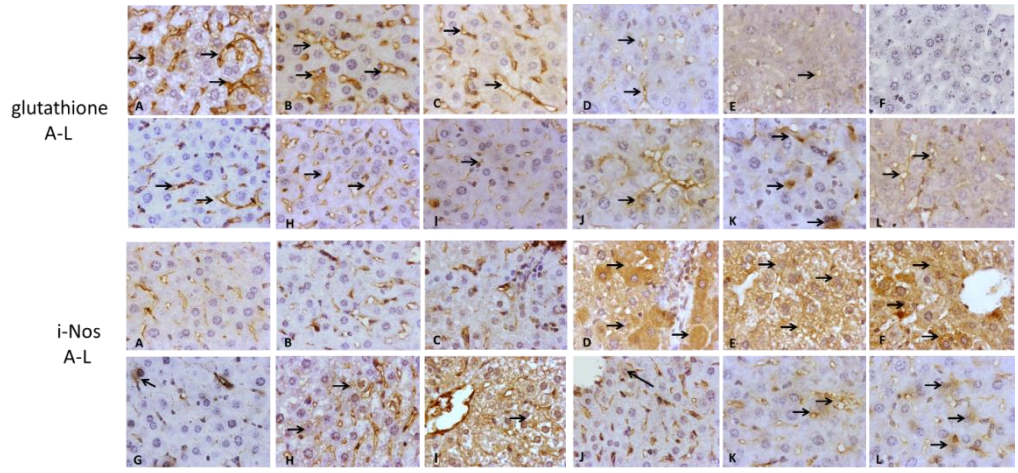

Fig 6. Representative IHC of GPx expression and localization in immunostained liver sections of different treatment groups A1-L1. A1) Livers of Group 1, B1) Group 2and C1) Group 3 showing strong brown immunopositive sinusoidal reaction. D1) Livers of Group 4, E1) Group 5 and F1) Group 6 showing decreasing immunopositive sinusoidal reaction with increased Cr dose. G1) Livers of Group 7 H1) Group 8 and I1) Group 9 showing decreasing immunopositive sinusoidal reaction with increased Cr dose. J1) Livers of Group 10, K1) Group 11 and L1) Group 12 showing decreased immunopositive sinusoidal reaction with increased Cr dose but appear higher than observed in unprotected groups and protected groups with cm0.5%. **Representative IHC of iNos expression and localization in immunostained liver sections of different treatment groups A2-L2.** A2) Livers of Group 1, B2) Group 2 and C2) Group 3 showing negative reaction. D2) Livers of Group 4, E2) Group 5 and F2) Group 6 showing increasing immunopositive reaction in hepatocytes with increased Cr dose. G2) Livers of Group 7, H2) Group 8 and I2) Group 9 showing increasing immunopositive reaction in hepatocytes. J2) Livers of Group 10, K2) Group 11 and L2) Group 12 showing increasing immunopositive reaction in hepatocytes with increased Cr dose but appears lower than in unprotected groups and protected groups with cm0.5%. Arrows point to immunopositive reaction. IHC counterstained with Mayer's hematoxylin. High magnification=400x.

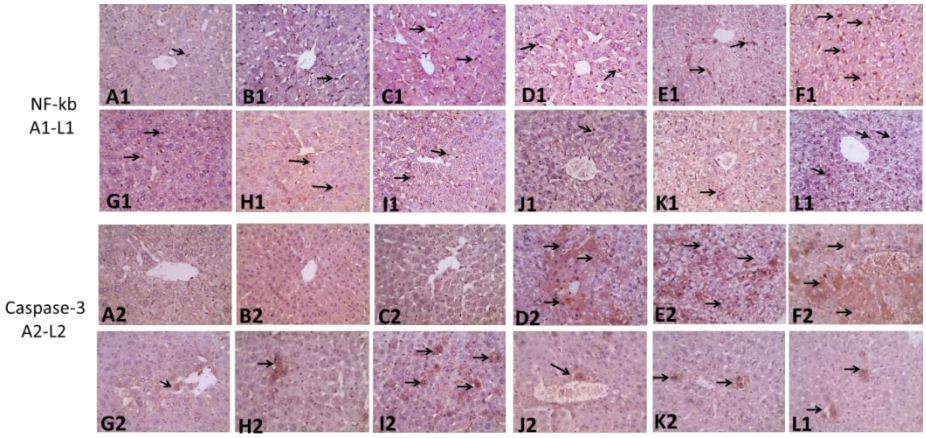

Fig 7. Representative IHC of NF-kb expression and localization in immunostained liver sections of different treatment groups A1-L1. A1) Livers of Group 1, B1) Group 2and C1) Group 3 showing few positively stained sinusoidal nuclei. D1) Livers of Group 4, E1) Group 5 and F1) Group 6 showing increasing immunopositive stained sinusoidal nuclei with increased Cr dose. G1) Livers of Group 4, H1) Group 5 and I) Group 6 showing increasing immunopositive stained sinusoidal nuclei with increased Cr dose. J1) Livers of Group 7, K1) Group 8 and L1) Group 9 showing slightly increased immunopositive stained sinusoidal nuclei with increased Cr dose but still lower than observed in unprotected groups and protected groups with cm0.5%. **Representative IHC ofcaspase-3 expression and localization in immunostained liver sections of different treatment groups A2-L2.** A2) Livers of Group 1, B2) Group 2 and C2) Group 3 showing negative reaction. D) Livers of Group 4, E2) Group 5 and F2) Group 6 showing increasing immunopositive reaction in hepatocytes with increased Cr dose. G2) Livers of Group 7, H2) Group 8 and I2) Group 9 showing increasing immunopositive reaction in hepatocytes. J2) Livers of Group 10, K2) Group 11 and L2) Group 12 showing increasing immunopositive reaction in hepatocytes that appears lower than in unprotected groups and protected groups with cm0.5%. Arrows point to immunopositive reaction. IHC counterstained with Mayer's hematoxylin. High magnification=400x.

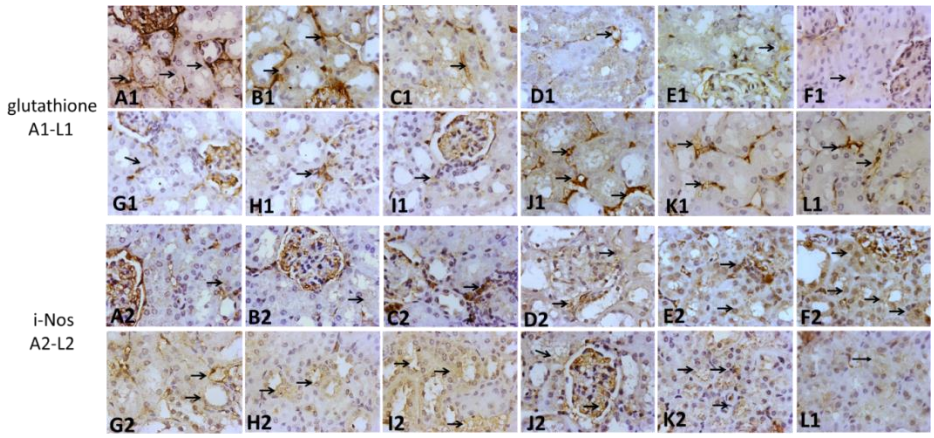

Fig 8. Representative IHC of GPx expression and localization in immunostained kidney sections of different treatment groups A1-L1. A1) Kidneys of Group 1, B1) Group 2 and C1) Group 3 showing strong immunopositive interstitial reaction. D1) Kidneys of Group 4, E1) Group 5 and F1) Group 6 showing decreasing immunopositive interstitial reaction with increased Cr dose. G1) Kidneys of Group 7, H1) Group 8 and I1) Group 9 showing decreasing immunopositive interstitial reaction with increased Cr dose. J1) Kidneys of Group 10, K1) Group 11 and L1) Group 12 showing decreased immunopositive interstitial reaction but still higher than observed in unprotected groups and protected groups with cm0.5%. **Representative IHC of iNos expression and localization in immunostained kidney sections of different treatment groups A2-L2.** A2) Kidneys of Group 1, B2) Group 2 and C2) Group 3 showing mild immunopositive tubular reaction. D2) Kidneys of Group 4, E2) Group 5 and F2) Group 6 showing increasing immunopositive tubular reaction with increased Cr dose. G2) Kidneys of Group 7 H2) Group 8 and I2) Group 9 showing increasing immunopositive tubular reaction with increased Cr dose. J2) Kidneys of Group 10, K2) Group 11 and L2) Group 12 showing increased immunopositive tubular reaction with increased Cr dose but still lower than observed in unprotected groups and protected groups with cm0.5%. Arrows point to immunopositive interstitial reaction. IHC counterstained with Mayer's hematoxylin. High magnification=400x.

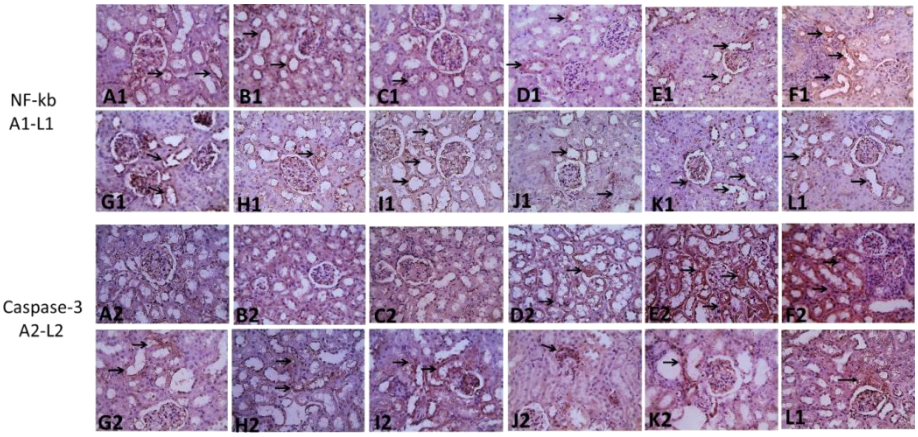

Fig 9. Representative IHC of NF-kb expression and localization in immunostained kidney sections of different treatment groups A1-L1. A1) Kidneys of Group 1, B1) Group 2 and C1) Group 3 showing mild immunopositive nuclear reaction in tubules. D1) Kidneys of Group 4, E1) Group 5 and F1) Group 6 showing increasing immunopositive nuclear reaction in tubules with increased Cr dose. G1) Kidneys of Group 7, H1) Group 8 and I1) Group 9 showing increasing immunopositive nuclear reaction in tubules with increased Cr dose. J1) Kidneys of Group 10, K1) Group 11 and L1) Group 12 showing increasing immunopositive tubular reaction with increased Cr dose but appear lower than observed in unprotected groups and protected groups with cm0.5%. **Representative IHC of caspase-3 expression and localization in kidney sections of different treatment groups A2-L2.** A2) Kidneys of Group 1, B2) Group 2 and C2) Group 3 showing mild immunopositive tubular reaction. D2) Kidneys of Group 4, E2) Group 5 and F2) Group 6 showing increasing immunopositive tubular reaction with increased Cr dose. G2) Kidneys of Group 7 H2) Group 8 and I2) Group 9 showing increasing immunopositive tubular reaction with increased Cr dose. J2) Kidneys of Group 10, K2Group 11 and L2) Group 12 showing increased immunopositive interstitial reaction with increased Cr dose but still lower than observed in unprotected groups and protected groups with cm0.5%. Arrows point to immunopositive reaction. IHC counterstained with Mayer's hematoxylin. High magnification=400x.

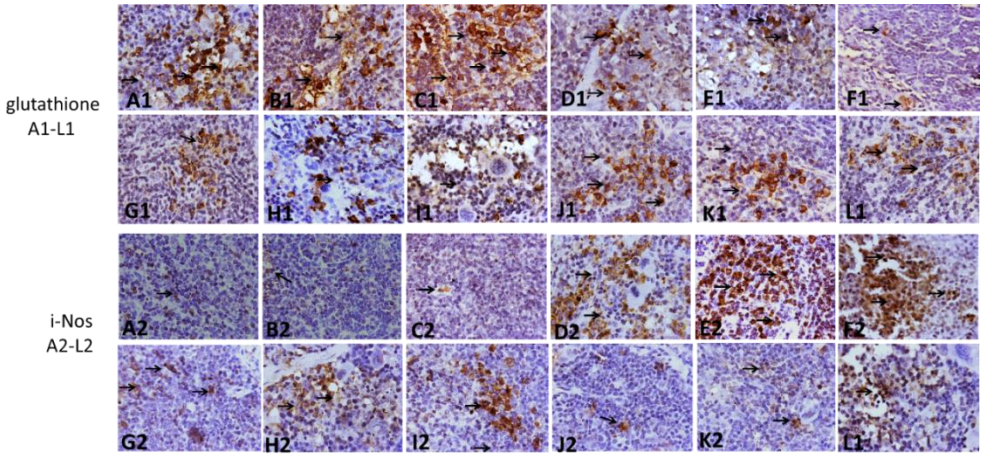

Fig 10. Representative IHC of GPx expression and localization in immunostained spleen sections of different treatment groups A1-L1. A1) Spleens of Group 1, B1) Group 2 and C1) Group 3 showing strong positive brown reaction in lymphocytes. D1) Spleens of Group 4, E1) Group 5 and F1) Group 6 showing decreasing immunopositive sinusoidal reaction with increased Cr dose. G1) Spleens of Group 7, H1) Group 8 and I1) Group 9 showing decreasing immunopositive brown reaction in lymphocytes with increased Cr dose. J1) Spleens of Group 10, K1) Group 11 and L1) Group 12 showing decreasing immunopositive brown reaction in lymphocytes with increased Cr dose but still higher reaction than observed in unprotected groups and protected groups with cm0.5%. **Representative IHC of iNos expression and localization in immunostained spleen sections of different treatment groups A2-L2.** A2) Spleens of Group 1, B2) Group 2 and C2) Group 3 showing negative reaction. D2) Spleens of Group 4, E2) Group 5 and F2) Group 6 showing increasing immunopositive reaction in lymphocytes with increased Cr dose. G2) Spleens of Group 7, H2) Group 8 and I2) Group 9 showing increasing immunopositive reaction in lymphocytes. J2) Spleens of Group 10, K2) Group 11 and L2) Group 12 showing lower immunopositive reaction in lymphocytes than in unprotected groups and protected groups with cm0.5%. Arrows point to immunopositive reaction. IHC counterstained with Mayer's hematoxylin. High magnification=400x.

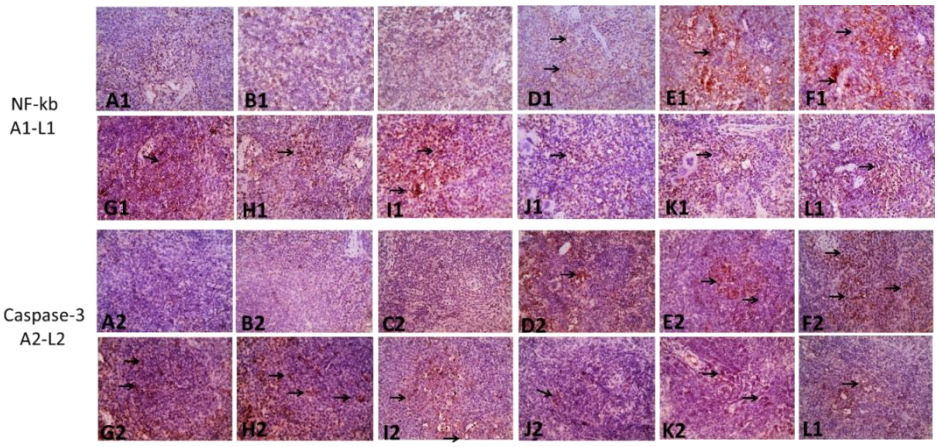

Fig 11. Representative IHC of NF-kb expression and localization in immunostained spleen sections of different treatment groups A1-L1. A1) Spleens of Group 1, B1) Group 2 and C1) Group 3 showing negative reaction. D1) Spleens of Group 4, E1) Group 5 and F1) Group 6 showing decreasing immunopositive reaction in lymphocytes with increased Cr dose. G1) Spleens of Group 7, H1) Group 8 and I1) Group 9 showing decreasing immunopositive in lymphocytes with increased Cr dose. J1) Spleens of Group 10, K1) Group 11 and L1) Group 12 showing higher immunopositive in lymphocytes than observed in unprotected groups and protected groups with cm0.5%. **Representative IHC of caspase-3 expression and localization in immunostained spleen sections of different treatment groups A2-L2.** A2) Spleens of Group 1, B2) Group 2 and C2) Group 3 showing negative reaction. D2) Spleens of Group 4, E2) Group 5 and F2) Group 6 showing increasing immunopositive reaction in lymphocytes with increased Cr dose. G2) Spleens of Group 7, H2) Group 8 and I) Group 9 showing increasing immunopositive reaction in lymphocytes. J2) Spleens of Group 10, K2) Group 11 and L2) Group 12 showing lower immunopositive reaction in lymphocytes than in unprotected groups and protected groups with cm0.5%. Arrows point to immunopositive reaction. IHC counterstained with Mayer's hematoxylin. High magnification=400x.

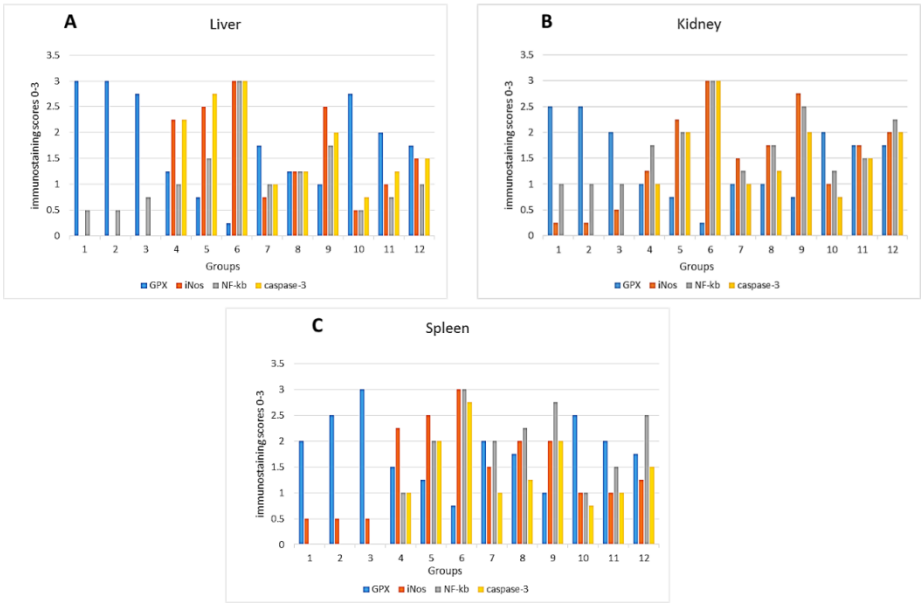

Fig 12. Statistical analysis of immunostaining scores in liver (A) kidney (B) and spleen (C) showing higher scores of GPX and lower scores of iNos, NF-kb, caspase-3 in three examined organs in groups protected with 2% cm than observed in than observed in unprotected groups and protected groups with 0.5% cm.

References

1. Dissawa, D.M.D.M. Effect of chlorothalonil on Drosophila melanogaster development and reproductive output. Macquarie University , (2024).
2. Van Scoy, A.R. and Tjeerdema, R.S. Environmental fate and toxicology of chlorothalonil. *Rev. Environ. Contam. Toxicol.*, **232**, 89-105 (2014).
3. Draper, A., Cullinan, P., Campbell, C., Jones, M. and Taylor, A.N. Occupational asthma from fungicides fluazinam and chlorothalonil. *Occup. Environ. Med.*, **60**(1),76–77 (2003).
4. Barreto, J.S., Tarouco, F.D.M., Godoi, F.G.A., Geihs, M.A., Abreu, F.E.L., Fillmann, G., Sandrini, J.Z. and Rosa, C.E. Induction of Oxidative Stress by Chlorothalonil in the Estuarine Polychaete Laeonereis Acuta. *Aquat .Toxicol.*, **196** , 1–8 (2018) .
5. Mahgoub, H.A., El-Adl, M.A.M. and Martyniuk, C.J. Fucoidan ameliorates acute and sub-chronic in vivo toxicity of the fungicide cholorothalonil in Oreochromis niloticus (Nile tilapia). *Comp. Biochem. Physiol. Part C Toxicol. Pharmacol.*, **245**, 109035 (2021).
6. Li, X., Yao, Y., Wang, S. and Xu, S. Resveratrol relieves chlorothalonil-induced apoptosis and necroptosis through miR-15a/Bcl2-A20 axis in fish kidney cells. *Fish. Shellfish .Immunol.*, **107**, 427-434 (2020).
7. Li, X., Zhao, x., Yao, Y., Guo, M. and Li, S. New Insights into Crosstalk between Apoptosis and Necroptosis Co-Induced by Chlorothalonil and Imidacloprid in Ctenopharyngodon Idellus Kidney Cells. *Sci. Total. Environ.*, **780** , 146591 (2021).
8. Wang, Y.S., Yang, S.J., Wan, Z.X., Shen, A., Ahmad, M.J., Chen, M.Y., Huo, L.J. and Pan, J.H. Chlorothalonil exposure compromised mouse oocyte in vitro maturation through inducing oxidative stress and activating MAPK pathway. *Ecotoxicol. Environ. Saf.*, **273**, 116100 (2024).
9. Vo, T.S., Vo, T.T.B.C., Vo, T.T.T.N. and Lai, T.N.H. Turmeric (Curcuma Longa L.): Chemical Components and Their Effective Clinical Applications. *Journal of the Turkish Chemical Society Section A: Chemistry* (*J.O.T.C.S.A.*), **3**, 883–898 (2021) .
10. Gupta, S.C., Kismali, G. and Aggarwal, B.B. Curcumin, a component of turmeric: from farm to pharmacy. *Biofactors.*, **39** (1),2–13 (2013) .
11. Heger, M., van Golen, R.F., Broekgaarden, M. and Michel, M.C. The molecular basis for the pharmacokinetics and pharmacodynamics of curcumin and its metabolites in relation to cancer. *Pharmacol .Rev.*, **66** (1),222–307 (2014) .
12. Shen, Y., Huang, H., Wang, Y., Yang, R. and Ke, X. Antioxidant Effects of Se-Glutathione Peroxidase in Alcoholic Liver Disease. *J. Trace. Elem. Med. Biol.*,**74** , 127048 (2022) .
13. Ahmad, A., Dempsey, S.K., Daneva, Z., Azam, M., Li, N., Li, P.L. and Ritter, J.K. Role of Nitric Oxide in the Cardiovascular and Renal Systems. *Int. J. Mol. Sci.*, **9**, 2605 (2018).
14. Papi, S., Ahmadizar, F. and Hasanvand, A. The Role of Nitric Oxide in Inflammation and Oxidative Stress. *Immunopathol .Persa.*, **5**(1) ,e08–e08 (2019).
15. Ben, P., Liu, J., Lu, C., Xu, Y., Xin, Y., Fu, J., Huang, H., Zhang, Z., Gao, Y., Luo, L. and Yin, Z. Curcumin degradation of inducible nitric oxide synthase and suppresses its enzyme activity in RAW 264.7 cells. *Int. Immunopharmacol.*, **11** (2), 179–86 (2011) .
16. Hariharan, A., Hakeem, A., Radhakrishnan, S., Reddy, M.S. and Rela, M. The Role and Therapeutic

Potential of NF-Kappa-B Pathway in Severe COVID-19 Patients. *Inflammopharmacology*., **29**, 91–100 (2021) .

17. Pérez, S.R., Pérez, S., Andrés, P.M., Monsalve, M. and Sastre, J. Nuclear Factor Kappa B Signaling Complexes in Acute Inflammation. *Antioxid. Redox. Signal*., **33**(3), 145–65 (2020) .

18. Lawrence, T. The nuclear factor NF-κB pathway in inflammation. *C.S.H. Perspect. Biol*.**,** **1** (6),a001651 (2009).

19. Guo, Q., Jin, Y., Chen, X., Xiaomin Ye, Xin Shen, Lin, M., Zeng, C., Zhou, T. and Zhang, J. NF-KB in Biology and Targeted Therapy: New Insights and Translational Implications. *Signal .Transduct. Target. Ther*., **1**, 53 (2024).

20 Cade, C.E. and Clark, A.C. Caspases–Key players in apoptosis. *Proteases apoptosis Pathways, Protoc. Transl. Adv*., 31–51 (2015).

21 Asadi, M., Taghizadeh, S., Kaviani, E., Vakili, O., Anganeh, M.T., Tahamtan, M. and Savardashtaki, A. Caspase-3: structure, function, and biotechnological aspects. *Biotechnol .Appl. Biochem*., **69** (4) , 1633–45 (2022).

22 Bhadra, K. A Mini Review on Molecules Inducing Caspase-Independent Cell Death: A New Route to Cancer Therapy. *Mol.*, **27**(19), 6401 (2022).

23. Council, N.R., Nutrition C on A, Nutrition S on LA. *N.R.C.*, 1995 (1995).

24. Jiao, Y., Wilkinson, I.V.J., Pietsch, E.C., Buss, J.L., Wang, W., Planalp, R., Torti, F.M. and Torti, S.V. Iron chelation in the biological activity of curcumin. *Free. Radic. Biol. Med*., **40** (7),1152–60 (2006).

25. Wang, Y., Jin, C., Wang, D., Zhou, J., Yang, G., Shao, K., Wang, Q. and Jin, Y. Effects of chlorothalonil, prochloraz and the combination on intestinal barrier function and glucolipid metabolism in the liver of mice. *J. Hazard. Mater.*, **410**,124639 (2021).

26. Farag, A.T., Karkour, T.A. and Okazy, A.El. Embryotoxicity of oral administered chlorothalonil in mice. *Birth. Defects .Res. B Dev. Reprod. Toxicol*., **77** (2),104–109 (2006).

27. Bancroft, J.D. and Gamble, M. Theory and practice of histological techniques. *Elsevier Health Sciences*., (2008).

28. Palipoch, S. and Punsawad, C. Biochemical and histological study of rat liver and kidney injury induced by cisplatin. *J .Toxicol .Pathol*., **26**(3), 293–9 (2013).

29. Handford, C.E., Elliott, C.T. and Campbell, K. A review of the global pesticide legislation and the scale of challenge in reaching the global harmonization of food safety standards. *I.E.A.M.*, **11** (4), 525–536 (2015).

30 Hamama, H.M. and Fergani, Y.A. Toxicity and oxidative stress induced in Spodoptera littoralis (Boisduval)(Lepidoptera: Noctuidae) treated with some insecticides. *Afr. Entomol*., **27** (2) ,523–531 (2019).

31 Curl, C.L., Fenske, R.A. and Elgethun, K. Organophosphorus pesticide exposure of urban and suburban preschool children with organic and conventional diets. *Environ. Health. Perspect*., **111** (3) ,377–382 (2003).

32 Garayzar, A.B.S., Bahamonde, P.A., Martyniuk, C.J., Betancourt, M. and Munkittrick, K.R. Hepatic gene expression profiling in zebrafish (Danio rerio) exposed to the fungicide chlorothalonil. *Comp. Biochem. Physiol. D*., **19**,102 , 11 (2016).

33 IPCS. WHO Recommended Classification of Pesticides by Hazard and Guidelines to Classification 2009. *W.H.O*., (2010).

34 Suttie, A.W. Histopathology of the spleen. *Toxicol.Pathol*., **34** (5),466- 503 (2006).

35 Dellal, I., Mallem, L. and Abdennour, C. Effect of chlorothalonil on renal activity of the male rat, (2020)(January).

36 Agarwal, R., Goel, S.K. and Behari, J.R. Detoxification and antioxidant effects of curcumin in rats experimentally exposed to mercury. *J. Appl .Toxicol*., **30** (5) ,457–68 (2010).

37 Hashish, E.A. and Elgaml, S.A. Hepatoprotective and nephroprotective effect of curcumin against copper toxicity in rats. *Indian. J. Clin .Biochem*., **31**, 270–7 (2016).

38. Liu, N., Li, J., Lv, J., Yu, J., Xie, J., Wu, Y. and Tang, Z . Melatonin alleviates imidacloprid phytotoxicity to cucumber (Cucumis sativus L.) through modulating redox homeostasis in plants and promoting its metabolism by enhancing glutathione dependent detoxification. *Ecotoxicol.Environ. Saf*., **217**,112248 (2021).

39. Lopes, F.C., Junior, A.S.V., Corcini, C.D., Sánchez, J.A.A., Pires, D.M., Pereira, J.R., Primel, E., Fillmann, G. and Martins, C.D.M.G. Impacts of the biocide chlorothalonil on biomarkers of oxidative stress, genotoxicity, and sperm quality in guppy Poecilia vivipara. *Ecotoxicol. Environ .Saf*., **188**,109847 (2020).

40. Li, X., Yao, Y., Wang, S. and Xu, S. Resveratrol relieves chlorothalonil-induced apoptosis and necroptosis through miR-15a/Bcl2-A20 axis in fish kidney cells. *Fish .Shellfish. Immunol*., **107**,427,434 (2020).

41. El-Bahr, S.M. Effect of curcumin on hepatic antioxidant enzymes activities and gene expressions in rats intoxicated with aflatoxin B1. *Phytother Res.*, **29** (1), 134–40 (2015).

42. Chico, L., Ienco, E.C., Bisordi, C., Gerfo, A.L., Schirinzi, E. and Siciliano, G. Curcumin as an ROS Scavenger in Amyotrophic Lateral Sclerosis. *React. Oxyg. Species.*, ***2***, 5 (2016).

43. Sugamura, K. and Keaney, Jr. J.F. Reactive oxygen species in cardiovascular disease. *Free. Radic. Biol. Med*., **51** (5),978–92 (2011).

44. Ferreira, M.L., Farinha, L.R.L., Costa, Y.S.O., Pinto, F.J., Disner, G.R., da Rosa, J.G. dos S. and Lima, C. Pesticide-induced inflammation at a glance. *Toxics*., **11** (11), 896 (2023).

45. Biswas, S.K. Does the interdependence between

oxidative stress and inflammation explain the antioxidant paradox? . *OXID. MED. CELL. LONGEV*., **2016**, 5698931 (2016).

46. Bhatt, D. and Ghosh, S. Regulation of the NF-KB-Mediated Transcription of Inflammatory Genes. *Front. Immunol*, , **5**,71 eCollection (2014).

47. Li, W., Suwanwela, N.C. and Patumraj, S. Curcumin by Down-Regulating NF-KB and Elevating Nrf2, Reduces Brain Edema and Neurological Dysfunction after Cerebral I/R. *Microvasc.Res*., **106**,117-127(2016) .

48. Manikandan, R., Beulaja, M., Thiagarajan, R., Priyadarsini, A., Saravanan, R. and Arumugam, M. Ameliorative effects of curcumin against renal injuries mediated by inducible nitric oxide synthase and nuclear factor kappa B during gentamicin-induced toxicity in Wistar rats. *Eur .J. Pharmacol*., **670** (2–3), 578–585 (2011).

49. Shishodia, S. Molecular Mechanisms of Curcumin Action: Gene Expression. *Biofactors.*, **39**(1) , 37–55 (2013).

50. Li, X., Zhao, X., Yao, Y., Guo, M. and Li, S. New insights into crosstalk between apoptosis and necroptosis co-induced by chlorothalonil and imidacloprid in Ctenopharyngodon idellus kidney cells. *Sci.Total. Environ*., **780**,146591 (2021).

51 Li, G., Chen, J.B., Wang, C., Xu, Z., Nie, H., Qin, X.Y., Chen, X.M. and Gong, Q. Curcumin protects against acetaminophen-induced apoptosis in hepatic injury. *World. J. Gastroenterol*., **19** (42), 7440 (2013).

الدور الوقائي للكركمين علي التغير النسيجي و الصبغات المناعية في كبد و طحال و كلي الفئران المعرضة لجرعات مختلفة من الكلوراثيونيل

هبه الله القصبي ، ولاء فكرى عوضين، ايمان عبد الوهاب وهبه الله محجوب

قسم الباثولوجيا، كلية الطب البيطري، جامعة المنصورة، المنصورة 35516 ، مصر.

المؤلف المراسل: ولاء فكرى عوضين، كلية الطب البيطرى، جامعة المنصورة، المنصورة 35516- مصر

الملخص

يستخدم الكلوروثالونيل في العديد من البلاد لحمايه المحاصيل من العدوى الفطرية .هذا المبيد الحشرى يحفز عمليه الاجهاد التاكسدي من خلال تثبيط الانزيمات المضاده للاكسده مثل انزيم الجلوتاثيون بيروكسيداز.الكوركمين وهو ماده طبيعيه مضاده للاكسدة ومستخرجة من جذور نبات الكركم . تم استخدام مائه وعشرون فأرة وزن 20-25 جرام في هذه التجربه وزعوا عشوائيا علي اثني عشر مجموعة بحيث ان كل مجموعه تحتوى علي عشره فئران. المجموعة الاولي: (مجموعة التحكم) تلقت الفئران العلف ومياه الصنبور. المجموعة الثانية: الفئران تلقّت كوركمين بنسبه نصف في المائه في العلف المقدم لها لمدة اثني عشر أسبوعاً. المجموعة الثالثة: الفئران تلقّت كوركمين بنسبة اثنين في المائه في العلف المقدم لها لمده اثني عشر أسبوعاً. المجموعة الرابعه : تلقت الفئران كلوروثالونيل بجرعه واحد من عشره ملجم لكل كجم من وزن الفئران في العلف لمدة خمسه أسابيع. المجموعة الخامسه: تلقّت الفئران كلوروثالونيل بجرعه عشره ملجم لكل كجم من وزن الفئران في العلف لمدة 5 أسابيع. المجموعة السادسه كلوروثالونيل بجرعه مائه ملجم لكل كجم من وزن الفئران في العلف لمدة 5 أسابيع. المجموعة السابعه : تلقّت الفئران كوركمين بنسبه نصف في المائه في العلف لمدة اثني عشر أسبوعًا تليها كلوروثالونيل بجرعه واحد من عشره ملجم لكل كجم من وزن الفئران في العلف لمدة 5 أسابيع. المجموعة الثامنه: تلقّت الفئران كوركمين بنسبه نصف في المائه في العلف لمدة اثني عشر أسبوعًا تليها كلوروثالونيل بجرعه عشره ملجم لكل كجم من وزن الفئران في العلف لمدة 5 أسابيع.المجموعة التاسعه : تلقّت الفئران كوركمين بنسبه نصف في المائه في العلف لمدة اثني عشر أسبوعًا تليها كلوروثالونيل بجرعه مائه ملجم لكل كجم من وزن الفئران في العلف لمدة 5 أسابيع. المجموعة العاشره :تلقت كوركمين بنسبه اثنين في المائه في العلف لمدة اثني عشر أسبوعًا تليها كلوروثالونيل بجرعه واحد من عشره ملجم لكل كجم من وزن الفئران في العلف لمدة 5 أسابيع.. المجموعه الحاديه عشره تلقت كوركمين بنسبه اثنين في المائه في العلف لمدة اثني عشر أسبوعًا تليها كلوروثالونيل بجرعه عشره ملجم لكل كجم من وزن الفئران في العلف لمدة 5 أسابيع. المجموعه الثانيه عشره : تلقت كوركمين بنسبه اثنين في المائه في العلف لمدة اثني عشر أسبوعًا تليها كلوروثالونيل بجرعه مائه ملجم لكل كجم من وزن الفئران في العلف لمدة 5 أسابيع. تمت عمليه القتل الرحيم للفئران بناءا علي المده المحدده لكل مجموعه ، وتم جمع عينات من أنسجة الكبد والكلى والطحال وحفظها في فورمالين بنسبة 10 ٪ لمدة 48 ساعة ثم تمريرها لعمل قوالب من شمع البارافين و تقطيعها و صبغها بصبغة الهيماتوكسلين و الايوسين للفحص الهيستوباثولوجي و صبغها مناعيا بعلامات لانزيم الجلوتاثيون بيروكسيداز و للانزيم المخلق لاكسيد النيتريك بيروكسيداز وللعامل النووي و للكاسباز-3. اظهر الكوركمين اثنين في المائه دورًا وقائيًا أكثر من النصف في مائه في حماية الثلاثة أعضاء التي تم فحصها ضد التاثير السام للمستويات المختلفة من الكلوروثالونيل من خلال زيادة نشاط انزيم الجلوتاثيون بيروكسيداز ، وتثبيط نشاط الانزيم المخلق لاكسيد النيتريك بيروكسيداز وللعامل النووي و للكاسباز-3 .

الكلمات الدالة: الكلوروثالونيل ، الكوركمين ، الفئران ، انزيم الجلوتاثيون بيروكسيداز ،الانزيم المخلق لاكسيد النيتريك بيروكسيداز ، العامل النووي و للكاسباز-3 .